Ad Hoc Networks 105 (2020) 102168

Contents lists available at ScienceDirect

Ad Hoc Networks

journal homepage: www.elsevier.com/locate/adhoc

Experimental evaluation of RSSI-based positioning system with low-cost LoRa devices

Andres Vazquez-Rodas*, Fabian Astudillo-Salinas, Christian Sanchez, Braulio Arpi, Luis I. Minchala

Department of Electrical, Electronics, and Telecommunications Engineering/Engineering Faculty, University of Cuenca, Av. 12 de abril 001, 010107 Cuenca, Ecuador

ARTICLE INFO

Article history:
Received 14 February 2020
Accepted 6 April 2020
Available online 7 May 2020

ABSTRACT

Along the last years, we have witnessed the growing demand for services, applications, and systems that depend on the specific location of both people and a variety of things and gadgets. Currently, the Global Positioning System (GPS) offers good accuracy on-location services around the world. Nevertheless, it does not work efficiently on applications that require several small, cheap, and low power devices. Under such conditions, researchers prefer to work with low-cost wireless alternatives such as WiFi, Zigbee, LoRa, Sigfox, among others. The purpose of this work is twofold. Firstly we evaluate the time-measurement and radio frequency capabilities of Pycom LoRa hardware implementation, in order to develop a low-cost and GPS-independent positioning system. Then, with these results, we propose and evaluate a positioning system with LoRa technology and based on the received signal strength indicator. Extensive field test measurements in outdoor rural environments show that we can obtain position estimation errors lesser than around 7% of the maximum distance between anchor nodes.

1. Introduction

Today, it is very important to localize people or objects for almost every life activity. Just to quote an example, in the commercial field, the location knowledge of the products of a company is fundamental to reduce the search and operation times, and as a result productivity is improved [1].

The most utilized location method around the world is the global positioning system (GPS). However, one the of main disadvantage of GPS is its high power consumption and cost, which prohibits its large-scale deployment [2]. Nowadays, new low cost and low power consumption wireless technologies are emerging, which allow the deployment of densely distributed networks for a wide range of applications. Among them, stands out environmental monitoring, humans, animals, or vehicles monitoring [3,4], athletes tracking [5], etc. In such applications, it is very important to optimize the power consumption and the total network deployment costs. In general, data rate requirements of such applications are less demanding. In this context, it is important to consider solutions based on the emerging low-power wide-area networks (LPWANs) which can efficiently operate over large areas and with battery-powered devices [6–8].

At present, the more relevant LPWANs are: LoRa [9], Sigfox [10], and NarrowBand IoT (NB-IoT) [11]. Many research works have shown the advantages of the new physical layer LoRa technolgy and its upper layer LoRaWAN complement regarding scalability, coverage, and energy efficiency [12,13]. From Neumann et al. [14] it is apparent that LoRa technology has greater potential to develop a positioning system alternative to GPS in comparison with the other LPWANs. Of course, other wireless technologies such as WiFi or Zigbee are useful for the development of low cost positioning systems.

On the other hand, the most common positioning algorithms are time of arrival (ToA), time difference of arrival (TDoA), angle of arrival (AoA), and received signal strength indicator (RSSI). Each of these algorithms requires that wireless devices present different features and hardware capabilities. Additionally, these last algorithms are complemented with the localization algorithms such as multilateration, triangulation, and trilateration.

On this basis, this work presents a deeper evaluation of a hardware implementation of LoRa technology, specifically the LoPy and FiPy devices of Pycom manufacturer. The evaluation focuses on the study of the time measurement capabilities of the devices in order to implement a time-based positioning system for real environ-

* Corresponding author.
E-mail addresses: andres.vazquezr@ucuenca.edu.ec (A. Vazquez-Rodas), fabian.astudillos@ucuenca.edu.ec (F. Astudillo-Salinas), chrispsan@hotmail.com (C. Sanchez), braulio.arpi.pc@gmail.com (B. Arpi), ismael.minchala@ucuenca.edu.ec (L.I. Minchala).

https://doi.org/10.1016/j.adhoc.2020.102168
1570-8705/

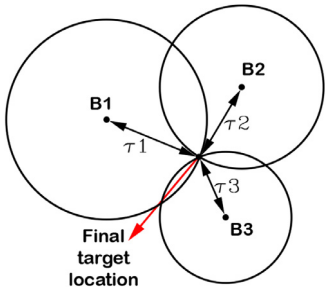

Fig. 1. ToA and RSSI position estimation approach.

ments. We also evaluate the quality of the radio frequency components in order to implement a positioning system based on RSSI variable. Finally, with these results, we implement and evaluate a low-cost RSSI-based positioning system. We evaluate the performance of the system through extensive field test measurements on outdoor rural environments of Cuenca-Ecuador.

2. Background

2.1. Positioning systems

Positioning systems can be broadly classified in one of the following categories: global positioning systems, which allows the localization of targets around the globe, or local positioning systems, which allow the localization of targets in a local environment of established size [15]. This work focuses on local positioning systems and this section presents a brief background on position estimation algorithms.

The time of arrival (ToA) position estimation algorithm gets the distance between the target node (TN) and each anchor node (AN) through the travel time measurements of the respective reference signals. Then, with a minimum of three anchor nodes with known positions and strict time synchronization, it is possible to localize the target node using a trilateration approach (Fig. 1). Meanwhile, the time difference of arrival (TDoA) estimation relaxes the synchronization requirements between the target node and the anchors, just anchor nodes must be synchronized. And in general, it overcomes the drawbacks of ToA.

In the angle of arrival (AoA) estimation, the anchor nodes estimate the target location based on the angle of the respective arriving signal. In a coplanar scenario, AoA requires just two anchor nodes, but they must be equipped with smart antenna arrays.

On the other hand, in the estimation based on the received signal strength indicator (RSSI), the anchor nodes estimate the target location mapping the RSSI with the distance traveled by the signal. It requires a path loss model to estimate such distance. Then, in the same way that ToA with a minimum of three anchor nodes the target node position is estimated by trilateration (Fig. 1) [15].

Path loss models are usually expressed in a logarithmic form as shown in Eq. (1) [16].

$$P_L(dB) = P_0 + 20\ \log\left(\frac{d}{d_0}\right) + X_\sigma \tag{1}$$

where:

d, is the transmission distance,

d_0, is the reference distance,

P_0, is the power strength at distance d_0,

X_σ, is usually a zero mean Gaussian distributed random variable of the received signal with standard deviation σ.

Another widely used model is the exponential decay model, shown in Eq. (2) [17]. This equation shows that path loss is an exponential function with frequency f and distance d. This equation was proposed for cases were the antennas are located near to trees and thus the signal propagates through the trees. Weissberger and COST-235 models are modifications of this model to different forested environments.

$$L(dB) = A\ f^B d^C \tag{2}$$

These models can be simplified into Eq. (3), as is proposed in [16].

$$P_L(dB) = a + b\ \log(d) + X_\sigma \tag{3}$$

In this case, all the characteristics of Eq. (2) are expressed in Eq. (3). The exponential factor of distance is b, and the other components are expressed by a. Both are adjusted by means of the values obtained in the measurement campaign. As in Eq. (1), the randomness of the received signal is expressed in X_σ. It is assumed that the error of fitting in Eq. (3) follows a Gaussian distribution with zero mean and standard deviation (σ). The standard deviation can be calculated between the fitted curve and the mean values of every measurement point as shown in Eq. (4).

$$\sigma = \text{std}(P_L - \text{FittedCurve}) \tag{4}$$

To calculate the P_L values from RSSI and SNR, Eq. (5) is used according to [18].

$$P_L = |\text{RSSI}| + \text{SNR} + P_{tx} + G_{rx} \tag{5}$$

While the received signal strength can be expressed as in Eq. (6)

$$\text{RSSI} = P_{tx} + G_{tx} + G_{rx} - P_L \tag{6}$$

Where, P_{tx} is the transmitted power in dBm, G_{tx} and G_{rx}, are the transmitter and receiver antenna gains respectively in dBi, and P_L represents the path loss model in dB.

Therefore, we can get the RSSI logarithmic model equation through a minimum squares fitting of the RSSI field measurements as in Eq. (7). Here, c and b, are constants.

$$y = c \times \ln x + b \tag{7}$$

For ToA and RSSI, in a 3D scenario, the target node location is determined by the intersection of all spheres, whose centers are the coordinates of the anchor nodes and the radii are the distances between the anchor nodes and the target node, Eq. (8).

$$(x - x_i)^2 + (y - y_i)^2 + (z - z_i)^2 = m_i^2,\ (i = 1, 2, \ldots, n) \tag{8}$$

Where (x_i, y_i, z_i) are the known coordinates of anchor nodes, m_i are the estimations of the distance between the anchors and the target node, and n is the number of anchor nodes. In this way, solving this equation, we get the target node coordinates (x, y, z). Then, the trilateration localization algorithm derives from this fundamental Eq. (8), which is the math basis for the ToA or RSSI based positioning systems. In the case of a 2D scenario with three anchor nodes, we get the system of second-order equations shown in Eq. (9).

$$\begin{cases} (x - x_1)^2 + (y - y_1)^2 = m_1^2 \\ (x - x_2)^2 + (y - y_2)^2 = m_2^2 \\ (x - x_3)^2 + (y - y_3)^2 = m_3^2 \end{cases} \tag{9}$$

In this work, we use an analytical model to solve this system of equations and to implement them in the proposed positioning system. Specifically, we use the variable changes of Eq. (10)

$$\begin{cases} x = x' + x_1 \\ y = y' + y_1 \end{cases} \tag{10}$$

Replacing Eq. (10) in Eq. (9), we obtain Eq. (11)

$$\begin{cases} x'^2 + y'^2 = m_1^2 \\ (x' + x_1 - x_2)^2 + (y' + y_1 - y_2)^2 = m_2^2 \\ (x' + x_1 - x_3)^2 + (y' + y_1 - y_3)^2 = m_3^2 \end{cases} \tag{11}$$

With the variable changes of the following Eq. (12)

$$\begin{cases} x'_2 = x_2 - x_1 \\ x'_3 = x_3 - x_1 \\ y'_2 = y_2 - y_1 \\ y'_3 = y_3 - y_1 \end{cases} \tag{12}$$

And replacing this variable changes of Eq. (12) in Eq. (11) we obtain the resulting linear system of equations of Eq. (13) ready to be implemented in the positioning system.

$$\begin{cases} x'x'_2 + y'y'_2 = \frac{1}{2}\left(m_1^2 - m_2^2 + {x'_2}^2 + {y'_2}^2\right) \\ x'x'_3 + y'y'_3 = \frac{1}{2}\left(m_1^2 - m_3^2 + {x'_3}^2 + {y'_3}^2\right) \end{cases} \tag{13}$$

This methodology could be extended for a two dimensional system with n number of anchor nodes, and following the preceding procedure, we can obtain the general linear system of equations shown in Eq. (14)

$$\begin{cases} x'x'_2 + y'y'_2 = \frac{1}{2}(m_1^2 - m_2^2 + {x'_2}^2 + {y'_2}^2) \\ x'x'_3 + y'y'_3 = \frac{1}{2}(m_1^2 - m_3^2 + {x'_3}^2 + {y'_3}^2) \\ x'x'_4 + y'y'_4 = \frac{1}{2}(m_1^2 - m_4^2 + {x'_4}^2 + {y'_4}^2) \\ \qquad\qquad \dots \\ x'x'_n + y'y'_n = \frac{1}{2}(m_1^2 - m_n^2 + {x'_n}^2 + {y'_n}^2) \end{cases} \tag{14}$$

It must be used the variable changes of Eq. (15)

$$\begin{cases} x'_2 = x_2 - x_1, \quad y'_2 = y_2 - y_1 \\ x'_3 = x_3 - x_1, \quad y'_3 = y_3 - y_1 \\ x'_4 = x_4 - x_1, \quad y'_4 = y_4 - y_1 \\ \quad \dots \\ x'_n = x_n - x_1, \quad y'_n = y_n - y_n \end{cases} \tag{15}$$

And the requested coordinates are found by Eq. (16)

$$\begin{cases} x = x' + x_1 \\ y = y' + y_1 \end{cases} \tag{16}$$

2.2. LoRa technology

Low power wide area networks (LPWANs) represent a new trend in the evolution of wireless communication technologies. This communication technology is able to connect and monitor high number of sensors, covering wide areas at low energy cost [19]. One of the newest approaches to this technology is long range (LoRa) [20]. LoRa gives all the LPWAN advantages, adding low device cost and easy deployment. LoRa-based wireless sensor networks (WSNs) are able to collect real time information such as temperature, rain, humidity, flow, among many others. One of the clear application scenario for LoRa is rural environments.

The general characteristics of an LPWAN network are:

- LPWAN requires a minimum energy consumption during operation. This is because the limited capacity of batteries and its high cost.
- Cost is an important factor. Especially in the nodes, easy-to-install tools must be provided, and both the hardware and software should be low-cost.
- Although the level of activity depends on the specific application, the device must be able to wake up only when be needed to send information. This point would support the idea of star type architectures against mesh architectures.
- The network infrastructure must be easy to assemble. The addition of devices or the transfer to other countries must comply with international standards.
- The transferred information between the node and the final user must be secure.

As previously stated, long range (LoRa) is currently one of the most relevant LPWAN technology. LoRa is a proprietary modulation scheme derived from the chirp spread spectrum modulation (CSS). Its main objective is to improve the sensitivity of the system at the cost of a reduction in the data rate for a given bandwidth (BW). LoRa implements variable data rates, using orthogonal spreading factors (SF). This allows a compromise between the data rate and coverage, as well as optimizing the performance of the network with a constant bandwidth.

LoRa is a physical layer implementation and as such, it is independent on higher layers. This allows it to coexist with different network architectures. Some basic concepts about LoRa modulation and the advantages to develop an LPWAN network are presented in [20]. Additionally, although the modulation of LoRa is patented, a rigorous mathematical signal processing description of the LoRa modulation and demodulation process can be found in [21].

In information theory, Shannon-Hartley theorem, defines the maximum rate at which the information can be transmitted on a communication channel with a specific bandwidth in presence of noise. From this well-known equation, it can be concluded that if it increases bandwidth, it can compensate the degradation of the signal-to-noise ratio (SNR) of the radio channel.

In direct sequence spread spectrum (DSSS), the transmitter carrier phase changes according to a code sequence. This process is achieved by multiplying the desired data signal with a spreading code, known as chip sequence. This chip sequence has a higher rate than the data signal, so widens the bandwidth of the original signal. As a result, a reduction in the amount of interference occurs due to a processing gain. DSSS is widely used in communication applications. However, there are challenges when it is necessary to reduce the cost and energy consumption of devices with this technology.

LoRa modulation solves the DSSS problems by providing an alternative of lower cost and lower energy consumption. In LoRa modulation, the spread spectrum is achieved by generating a chirp signal that continuously varies in the frequency domain. An advantage of this method is that the timing and frequency variations between the transmitter and the receiver are equivalent, reducing the receiver complexity.

This chirp bandwidth is equivalent to the spectral signal bandwidth. The desired signal is widened with a chip and modulated on a chirp. The relationship between the desired data rate, the symbol rate and the chip rate for LoRa, is expressed by the Eq. (17).

$$R_b = SF \frac{\text{CodeRate}}{\frac{2^{SF}}{BW}} \text{ [bps]} \tag{17}$$

where:

- R_b is the bit rate of the modulation
- SF corresponds to the spreading factor, and could be in the range $(7 - 12)$
- CR is the code rate option $(1 - 4)$
- BW represents the bandwidth in [Hz]
- CodeRate $= 4/(4 + CR)$

2.2.1. LoRa transmission parameters

LoRa devices can be configured using different Transmission Power (TP), Carrier Frequency (CF), Spreading Factor (SF), Bandwidth (BW) and Coding Rate (CR). This parameters are tuned to achieve the best connection performance and the lowest energy consumption.

The previous variables combination results in around 6720 possible configurations, which allows a user to completely adjust LoRa

to the required application [22]. Next, a brief description of the mentioned parameters is presented [23]:

1. **Transmission Power (TP)**: It can varies between −4 dBm and 20 dBm, but due to implementation limits, it can be adjusted from 2 dBm to 20 dBm. With transmission power of more than 17 dBm, only 1% of the duty cycle can be used.
2. **Carrier Frequency (CF)**: It is the central frequency that can be varied in 61 Hz steps between 137 MHz and 1020 MHz, depending on the chip and the region of use.
3. **Spreading Factor (SF)**: It is the ratio between the symbol rate and the chip rate. A higher SF not only increases the SNR, range and sensitivity, but also the air time of the packet. Each increase in the SF reduces the transmission rate, doubling the duration of the transmission and the energy consumption. The SF can vary between 6 and 12, being useful for network separation since the SFs are orthogonal.
4. **Bandwidth (BW)**: It is the frequency range in the transmission band. A higher BW gives a higher data rate (less airtime), but lower sensitivity for noise aggregation. A lower BW requires more precise crystals, that is, less parts per million (ppm). The data is sent at a chip rate equivalent to the BW. A BW of 125 kHz is equivalent to a chip rate of 125 kcps. A typical LoRa network operates at: 125 kHz, 250 kHz or 500 kHz.
5. **Code Rate (CR)**: It is the Forward Error Correction rate (FEC) used by LoRa against interference. It can be configured with: 4/5, 4/6, 4/7 and 4/8. A larger CR offers more protection against noise, but increases the airtime. Transmitters with different CR can communicate since the CR is in the header of the packet that is always encoded at a 4/8 rate.

2.2.2. Key LoRa modulation properties

In the following we describe some key aspects that highlight LoRa and make it one of the best candidates for IoT applications [20]:

- **Scalable Bandwidth**: It can be used in narrow band frequency jumps and broadband direct sequence applications.
- **Low Energy Consumption**: Power output can be reduced compared to FSK, while keeping the same or better link budget.
- **High Robustness**: Due to its asynchronous nature, the LoRa signal is resistant to in-band and out-band interference.
- **Fade Resistant**: Thanks to the broadband chirp pulses, LoRa offers fading and multipath immunity, making it ideal for urban and suburban environments.
- **Doppler Resistant**: Doppler shift causes a small frequency shift in the LoRa pulse that introduces a non significant time axis shift of the baseband signal, making it immune to the Doppler effect.
- **Wide Coverage Capability**: Compared to FSK, maintaining the same transmission power, the link budget is higher in LoRa.
- **Enhanced Network Capability**: SemTech LoRa modulation employs orthogonal SFs that allow multiple propagation signals to be transmitted at the same time and on the same channel without substantial sensitivity degradation. The modulated signals with different SFs appear as noise to the target receiver and can be treated as such.

3. Related work

As low power wide area networks, and specifically LoRa technology become more popular, many researchers around the world focuses on evaluate the performance of such technology through experimental studies. For instance, in [24] authors present a test-bed for the study of a University campus IoT network using LoRa. They focuses on link quality and transmission performance evaluation. In [25] the performance of LoRa technology under two or more concurrent transmissions is evaluated. In [26], authors evaluate the performance of the LoRaWAN protocol by means of a permanent outdoor test-bed. The main objective is to evaluate the impact of the adaptive data rate scheme, the payload length, and the acknowledgments over the packet delivery ratio. The RSSI and SNR variables analysis shows the LoRa high sensitivity. The measured RSSI values are between −125 dBm and −78 dBm, while the extreme values for SNR are between −19.2 dB and 12.8 dB. Kazdaridis et al. [27] present the evaluation of LoRa performance using a test-bed deployed in the city of Volos, Greece. The system evaluate, under realistic conditions, the link quality by continuously monitoring the packet delivery ratio versus the RSSI relation. In [28] authors evaluate LoRa fading characteristics, coverage, and energy consumption in multi-floor indoor buildings. For smart city applications, in [29] authors present an experimental evaluation of LoRaWAN technology under real conditions in the city of Brno, Czech Republic. End-nodes use an Arduino Mega micro-controller with a RN2483 radio modules. The obtained values for RSSI ranges from -111 dBm to -64 dBm. The work in [30] presents a monitoring network based on LoRa connectivity to measure structural displacements of the medieval City Walls in the city of Siena, Italy.

On the other hand, several recent works focus on the implementation of low-cost and energy efficient positioning systems based on LoRa technology. For example, authors in [31] propose an hybrid LoRa-GPS tracker for dementia patients. Users incorporate LoRa appliances as end systems. The main objective of this work is to improve the energy efficiency of the GPS system by integrating LoRa communications and using a GPS duty cycling strategy. In [32] authors propose a TDoA LoRa positioning system which uses a multilateration location algorithm. Although authors entitle their proposal as GPS-free geolocation, the end-nodes and the gateways incorporate GPS for synchronization purposes. This work presents an accuracy of around 100 m in a 2 km × 2 km urban area. The LoRa Alliance in [33] presents a compilation of technical capabilities of LoRaWAN-based geolocation. The work focuses on new generation of LoRaWAN gateways which incorporate TDoA positioning algorithm capabilities. Paper also include real deployment case studies, with this specialized high cost gateways, in Barcelona port, urban environment of Issy-les-Moulineaux, Bolougne next to Paris, among others. In [34] authors provide experimental quantification of TDoA geolocation performance for outdoor tracking purposes using a public LoRaWAN network in Netherlands. Using six LoRa nodes configured with spreading factors between 7 and 12, and a single gateway, authors found that the median error of the raw TDoA location was around 200 m and in 90% of the cases the error was less than 500 m. In [35] authors propose a LoRa-based long range emergency communication system. The aim is to be a support for survivors and rescue teams and it is intended for critical environments where there is no cellular coverage and the common GPS-based localization is not completely available. Authors include simulation an experimental evaluation of the capabilities of the LoRa-based trilateration technique. For smart farming, one of the possible applications of our proposal, authors in [36] propose an agro-industry platform intended for monitoring, traceability and optimization of farming resources and processes. It includes WiFi-based localization for detecting anomalous behavior patterns of animals. In this line, a review of communication technologies for precision agriculture, which includes LoRa can be found in [37].

Our proposal strongly depends on precise path loss modeling, regarding this, our workgroup presents in [38] a methodology to experimentally study LoRa transmission range based on path-loss modeling, and through RSSI and SNR measured variables on real environments in the City of Cuenca, Ecuador. Other works related to propagation and coverage measurements are summarized in the following. In [18], authors present a study of performance and coverage that uses LoRa transceivers and RSSI as the main measure-

ment variable to develop a path loss model. The study is conducted in water and a coast environment. Authors use European 868 MHz ISM band. Another outdoor measurement based study is presented in [39], where the authors use PER and RSSI to estimate the performance of the system under two different tests. Authors evaluate the system under different payload length, bandwidth, spreading factor, and modulation schemes. The work uses different payload lengths, transmission with the FSK modulation scheme, and the Fresnel zone is taken into account. The work in [40], presents a general evaluation of LoRa using multiple gateways, RSSI and ACKs to estimate the connection rate. A main aspect of the study is the reliability that was measured using long transmission periods. The study detected mobile network interference during certain hours. Indoor measurements have been conducted in [41] and [42]. In [41], DR, SF, bandwidth and bit rate are fixed and RSSI is used to measure performance. In [42], the study is more specific, the authors evaluated the performance of LoRa in health and wellbeing applications.

This work focuses on a deeper evaluation of the capabilities of low cost Pycom LoRa hardware implementation, in order to develop a totally GPS-independent positioning system. We also include the performance evaluation of a RSSI-based positioning system through extensive field test on rural and open environments. An important remark is that most of the experimental studies reported in the literature were conducted on cities that are a few meters above the sea level. In this work, the evaluation was done in the southern Ecuadors Andes mountains at an altitude of around 2660 m above sea level.

4. Methodology

To develop a GPS-independent positioning system using low cost Pycom LoRa devices, firstly it is necessary to evaluate the behavior and performance of such devices under real environments. The proposed system could be based on time or RSSI variables, as stated in the Background section. For the time-based positioning, we require to evaluate the time measurement capabilities. To perform this evaluation we search different ways to measure and estimate the round trip time (RTT). For the system based on RSSI, in first place, we evaluate at laboratory in a controlled environment the RSSI sensitivity and the dynamic range. Another important parameter is the transmission power, the evaluation of this parameter has been executed using a National Instruments PXI system. Finally, we analyze the resulting positioning system through extensive measurement campaigns.

The positioning proposal based on the RSSI and the trilateration location algorithm has been evaluated by measurement campaigns. The measurement interval is based on spatial averaging. The authors of [38,43] defined a suitable measurement interval between 20λ and 40λ. The available LoRa device works in the 915 MHz ISM band. The corresponding lower and upper distance for this band are 6.5573 m and 13.1147 m. We select an integer value between the lower and upper limit. The chosen value was 10 m.

The behavior of the RSSI variable is evaluated in several locations of the Cuenca City in Ecuador. The goal is to identify locations that present stable and reliable results for the characterization of the path loss model. The PLM is used to estimate the location of the target node in the positioning system. The main feature of the location is that it covers a large open area. This area will allow LoS communication between all devices. We selected three main locations for the tests:

- Location 1 (Fig. 2(a)): Soccer field of the University of Cuenca ($2°54'7.63''S$; $79°0'41.20''O$). The terrain is flat with total LoS and with approximate dimensions of 150 × 150m.
- Location 2 (Fig. 2(b)): Pachamama plateau of the Cuenca city ($2°49'58.72''S$; $78°55'43.75''O$). It is a flat terrain with total LoS and with an approximate dimension of 500 × 500m.

(a) Location 1: Soccer field in the University campus

(b) Location 2: Pachamama plateau

(c) Location 3: Irquis farm

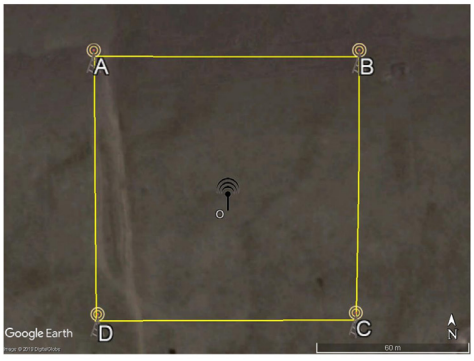

(d) Anchors location

Fig. 2. Test locations.

Table 1
Description of the test scenarios of the positioning system.

Type	Description
Symmetric	Scenario 1: 90 × 90m
	Scenario 2: 150 × 150m
Non-symmetric	Scenario 3: with error introduced, distances ≥ 100m
	Scenario 4: without error introduced, distances < 100m

- Location 3 (Fig. 2(c)): Irquis Farm of the University of Cuenca ($3^{\circ}4'49.20''S$; $79^{\circ}4'31.26''O$). It is a flat land with total LoS and with an approximate dimension of 200 × 200m.

Several tests have been performed to evaluate the system at each location. The tests consist of establishing communication links between FiPy and/or LoPy devices to assess the behavior of the system. For all locations, it has been measured the RSSI in function of the distance. The measurement interval was the previously defined 10 m.

At first stage, the variables RSSI and SNR are acquired and stored. The outbound link is measured in the anchor node and stored in the target node. The return link is measured and stored in the target node. As second stage, the null RSSI values are filtered. These values are given when the transmission is not completed.

Some evaluation scenarios have been established, with certain differences between them. Such different parameters to configure the scenarios are the number of anchor nodes, distances between anchor nodes, and RSSI characterization approaches. The aim of the study is to evaluate the position estimation errors for each case. The position error is evaluated by both, through simulations and by real measurements.

The measurements has been taken in an open area with no obstacles. We defined two types of scenarios: symmetric and not symmetric. These scenarios differ in the geometric distribution of anchor nodes. In symmetric type scenario, anchor nodes have a regular square distribution (Fig. 2(d)). In the non-symmetric type scenario, the distribution of anchor nodes is random. Table 1 lists the analyzed scenarios. There are three scenarios of symmetric type and two scenarios of non-symmetric type.

5. Performance evaluation of LoRa device capabilities

The purpose of this section is to evaluate the performance of LoPy and FiPy LoRa devices regarding their time measurement capabilities, RSSI sensitivity, and dynamic range.

5.1. LoPy and FiPy devices description

LoPy and FiPy are low-cost development boards produced by Pycom manufacturer, which include LoRa technology [44]. Table 2 summarizes the more relevant technical features of these boards. Besides, these devices have incorporated a 150kHz real-time clock (RTC) and a RSSI sensitivity sensor. In this section, we evaluate the real performance of these two last characteristics through field measurements. The goal is to determine if they are suitable for either time or RSSI based positioning system.

Table 2
Technical features of LoPy and FiPy devices [45,46].

Feature	LoPy 1.0 and FiPy
RTC (kHz)	150
ISM bands (MHz)	868, and 915
Semtech [47] chip	SX1272
Range (MHz)	860 – 1020
SF	6 – 12
BW (kHz)	125 – 500
Data Rate (kbps)	0.24 – 37.5
RSSI sensitivity (dBm)	−117 to −137

Table 3
RSSI Sensitivity of LoPy and FiPy devices [45,46].

BW (kHz) and SF	LoPy 1.0 (dBm)	FiPy (dBm)
125 and 6	−121	−122
250 and 12	−134	−135
500 and 12	−129	−131

It is important to note that the RSSI sensitivity of the LoRa devices vary in function of the operation bandwidth (*BW*) and spreading factor (*SF*). In this context, Table 3 presents the RSSI sensitivity of LoPy and FiPy devices under different BW and SF configurations.

5.2. Evaluation of LoPy and FiPy time measurement capabilities

Time-based positioning algorithms such as ToA or TDoA have strict requirements regarding the time measurement capabilities of the devices. For LoPy and FiPy boards we identify and evaluate three different ways to measure and estimate the round trip time (RTT): (1) through the built-in chronometer function, (2) using the internal RTC, and (3) through the CPU instruction or cycle time.

In order to evaluate and compare the real time measurement capabilities of LoPy and FiPy devices, we develop a set of field tests in which we establish a communication link between the target node and one anchor node. We measure the RTT for three different distances (15m, 2.6km, 10km) between the target and anchor nodes. For each evaluation point, the target node sends a message, then the anchor replies with an echo. After that, the target measures and estimates the RTT using one of the previously mentioned evaluation methods. In order to present reliable results, the target node repeats the experiment around 200 times for each point and we report the average RTT with 95% confidence interval.

Fig. 3 compares the resulting RTT estimation using the chronometer function, the internal RTC, and the CPU cycle method respectively. From this figure, we can conclude that, with these low-cost devices, no one of the RTT estimation methods present suitable results for a time-based positioning system development. We can observe an overlapping of confidence intervals of the measured RTT for all the cases with the chronometer function estimation. We can also see that the built-in chronometer function presents more variable results in comparison with the other two methods. Finally, for RTC and CPU cycle we can observe also an overlapping of the confidence intervals of the RTT between the measurements at 15m and the measurements at 2.6km, and a slight time difference for the 10km distance.

5.3. Evaluation of RSSI sensitivity and dynamic range

LoPy and FiPy devices allow the configuration of their LoRa modulation RF features such as: transmission power (P_{TX}), bandwidth, and spreading factor. As expected, these different configuration possibilities have a direct impact on the device RSSI sensitivity, as reported by the manufacturer in Table 3. Accordingly, in this section we evaluate the real dynamic range and sensitivity of LoPy and FiPy devices through controlled field tests.

The controlled field test consists of establishing a communication link between a LoPy 1.0 transmitter and other LoPy 1.0 receiver. In order to control the attenuation of the transmission power, the LoPy transmitter is connected to a Hewlett Packard (HP) 8496B variable attenuator (Fig. 4). This HP attenuator has a resolution of 1dB, and its attenuation ranges from 1 to 121dB.

We evaluate the LoPy RSSI behavior under two different configurations of P_{TX}, *BW*, and *SF*. The first set of tests was done

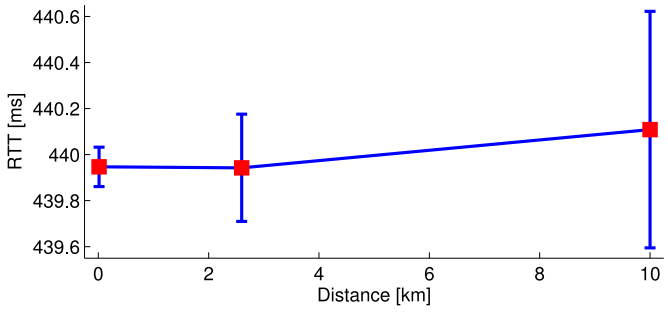

(a) Built-in chronometer function.

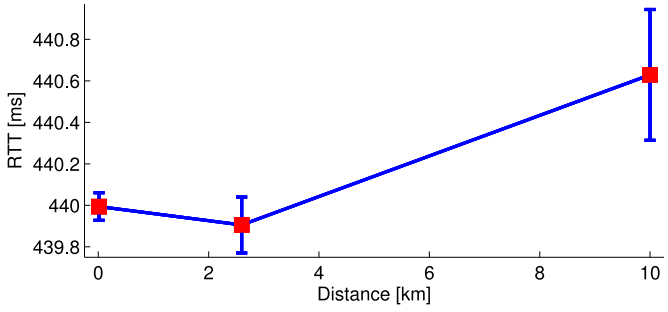

(b) RTC.

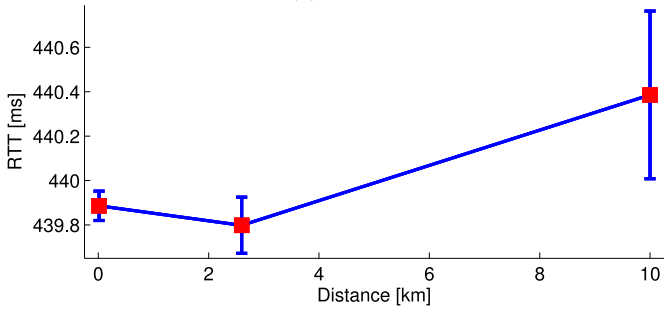

(c) Ticks, instruction time or CPU cycle.

Fig. 3. Performance results of three different methods of RTT measurements, with BW= 500kHz, SF = 12 and $P_{TX} = 20$dBm.

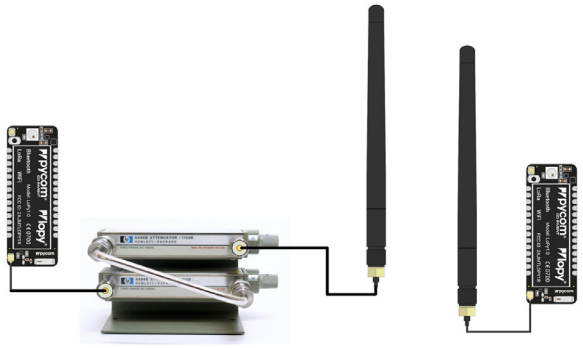

(a) T_X device with variable attenuator. (b) R_X device.

Fig. 4. Dynamic range tests of RSSI sensitivity.

with $BW = 500$kHz, and $SF = 12$. In turn, the second set used a $BW = 125$kHz, and a $SF = 7$. In both cases we evaluate the system configured with the minimum and the maximum allowed transmission power corresponding to 5 dBm and 20 dBm respectively. Furthermore, we establish and evaluate three different separation distances between the transmitter and the receiver ($d = 10$m, $d = 30$m, and $d = 50$m). In turn, for each separation distance, we vary the attenuation from 0dB to 50dB with 5dB steps.

Fig. 5 shows the resulting RSSI value evolution measured by the receiver node, for each described test. From Fig. 5(b), in first

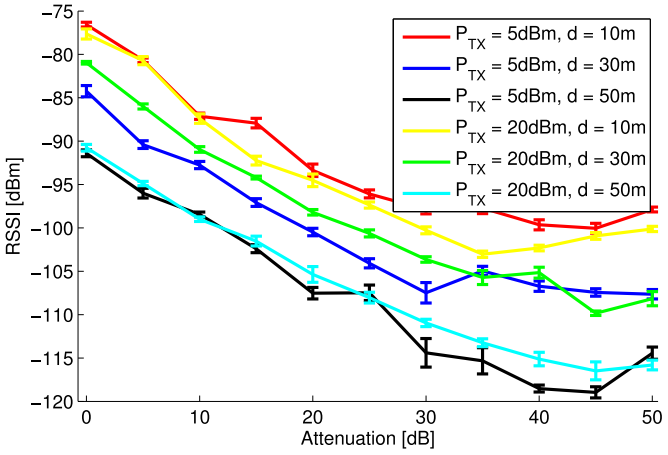

(a) Test 1 with $BW = 500$ kHz and $SF = 12$.

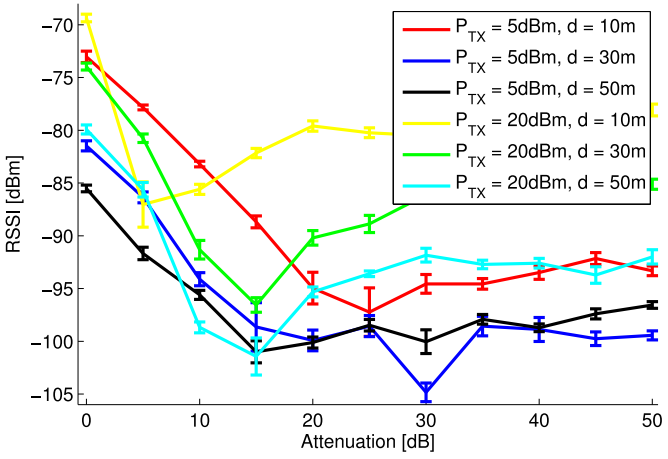

(b) Test 2 with $BW = 125$ kHz and $SF = 7$.

Fig. 5. Field controlled tests of links between a LoPy 1.0 as T_X with variable attenuator and other LoPy 1.0 as R_X.

place, we can observe that when the system is configured with $BW = 125$kHz, and a $SF = 7$ the behavior of the RSSI is more unpredictable and so the dynamic range in this case is not clear. Thus, this configuration does not allow to have a good characterization of the communication link between the transmitter and the receiver. Then, this configuration is not suitable for a RSSI-based positioning system. On the other hand, for the system configured with $BW = 500$kHz, and $SF = 12$, on Fig. 5(a), we observe a stable behavior of the RSSI variable for all the cases until an attenuation of around 30dB, which corresponds to a RSSI value greater than around -110 dBm. This implies that the dynamic range of LoPy devices is suitable for a RSSI-based positioning system development for values of RSSI greater than -110 dBm and when the LoRa modulation is configured with $BW = 500$kHz, $SF = 12$ and $P_{TX} = 5$ dBm.

Another observation from the field tests is the fact that different LoPy and FiPy devices, in spite of using the same chip Semtech SX1272 [47], exhibits different behaviors regarding RSSI sensitivity and dynamic range. Additionally we expect a greater impact of the selected transmission power over the resulting RSSI values. These two facts motivated us to make a deeper analysis of the real transmission power of the LoPy and FiPy devices and its variability.

5.4. Evaluation of the transmission power

In order to make a deeper and reliable evaluation of the LoPy and FiPy devices transmission power, we use as a receiver a National Instruments PXI system. For this test set, the LoPy or FiPy

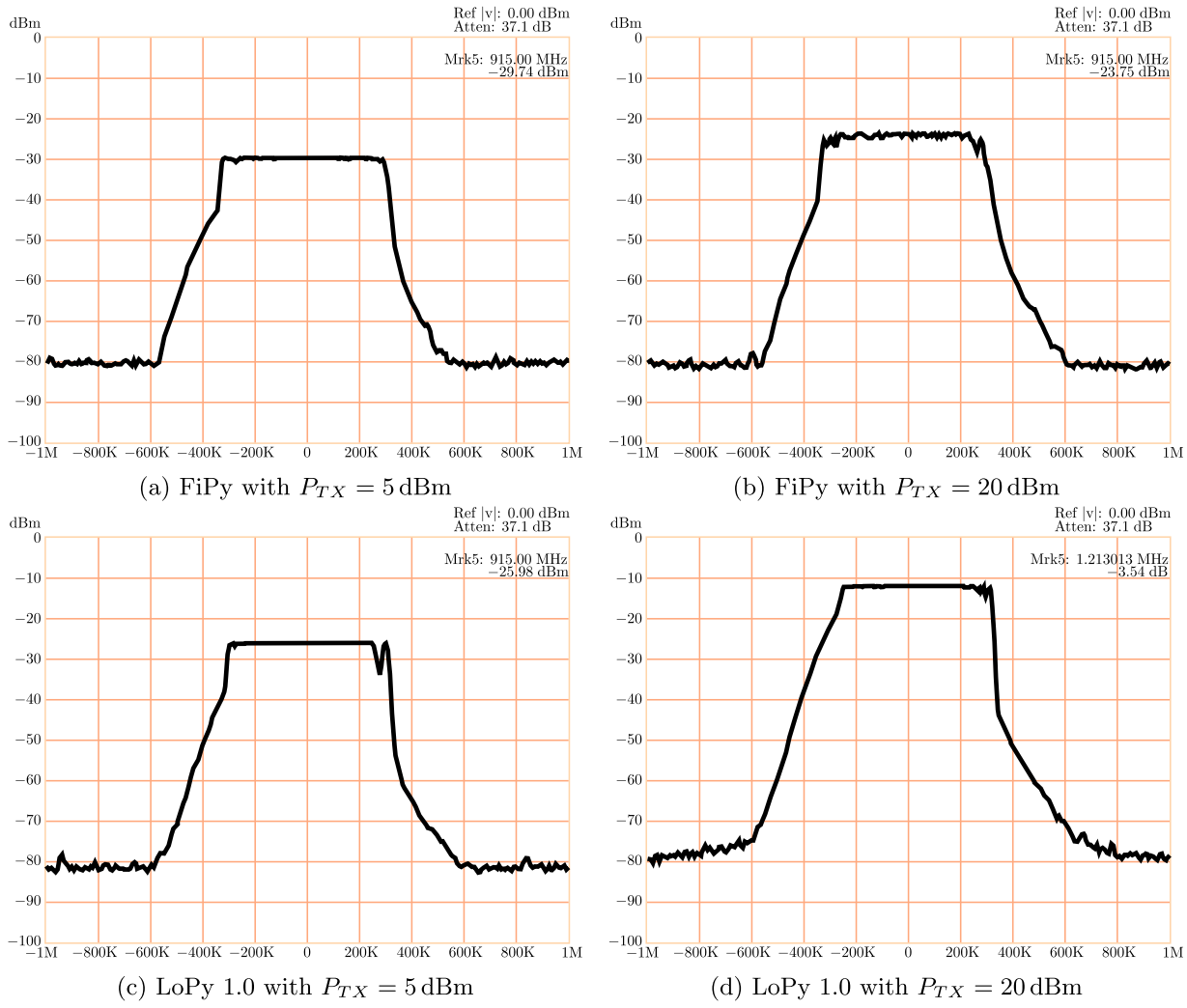

Fig. 6. Power transmission evaluation of LoPy and FiPy devices with BW= 500 kHz, SF= 12 and 30 dB of attenuation.

transmitter is connected to the attenuator configured with an attenuation value of 30dB to guarantee that the power keeps in the range accepted by the PXI receiver module. Each device is evaluated for its minimum ($P_{TX} = 5$ dBm) and its maximum ($P_{TX} = 20$ dBm) transmission power.

The first test was done with a FiPy device configured with the following LoRa modulation parameters: $P_{TX} = 5$ dBm and $BW = 500$ kHz. Since we use an attenuation of 30dB we expect that the received power in the PXI system to be around −25 dBm. However, as it can be observed in the Fig. 6(a), the real received power is −29.74 dBm. Thus for this FiPy device we obtain a power error of −4.74 dBm. We also observe a real transmission bandwidth of $BW = 608.97$ kHz. Then, it is around of 108.97 kHz out of band emission.

In the second case, the FiPy device was configured with $P_{TX} = 20$ dBm and $BW = 500$ kHz. Fig. 6(b) presents the resulting power and *BW* reported by the PXI for this configuration. We observe a received power of -23.75 dBm, so an error of -13.75 dBm is obtained. Thus, when the device is configured with the maximum transmission power, the error of the power amplifier is significantly increased. Regarding the *BW* error it remains the same as the previous case (108.97 kHz).

In turn, for the LoPy device configured with $P_{TX} = 5$ dBm and $BW = 500$ kHz, the resulting power error is around −0.94dBm as it is depicted in the Fig. 6(d). The measured *BW* is 528.84kHz so the obtained error is 28.84 kHz. Finally, when the LoPy device is configured with the maximum transmission power $P_{TX} = 20$ dBm and BW= 500 kHz, the power error is −1.97dBm as it can be see in the Fig. 6(c). For this last case the measured transmission *BW* is 520.83 kHz and therefore we obtain a 20.83kHz of out of band emission.

Therefore, we can conclude that the radio frequency components of LoPy 1.0 devices and its RF accessories are of better quality than the FiPy devices. Also, in order to have a better behavior of the positioning system, the preferred configuration of LoRa modulation parameters for this kind of devices is $BW = 500$ kHz, $SF = 12$, $P_{TX} = 5$ dBm, preamble equal to 8 and $CR = 4/5$.

6. RSSI-Based positioning system

Based on the LoPy and FiPy devices detailed evaluation presented in the Section 5, in this section we start defining the proposed RSSI-based positioning system architecture and then we present the performance evaluation of the system.

6.1. System architecture

For the proposed positioning system, we choose an architecture centralized on the target node. We do not use any specialized gateway, with dedicated localization features, with the purpose of keep at the minimum the system costs. Then, in such architecture, the target node establishes a communication link with each anchor

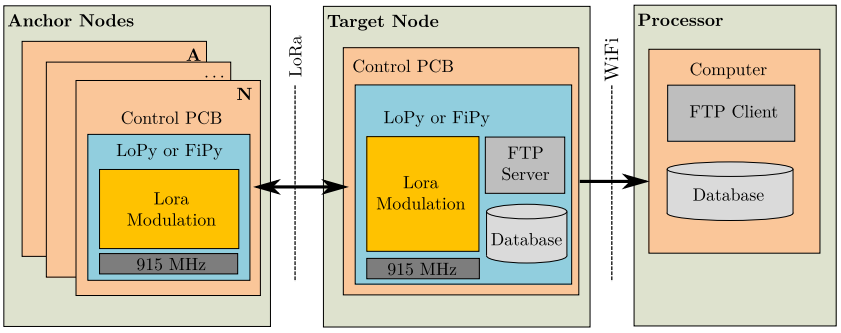

Fig. 7. General Architecture.

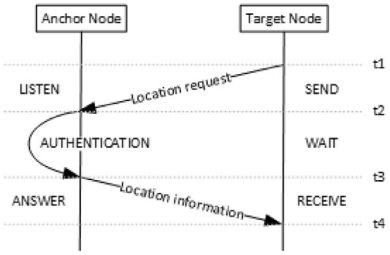

Fig. 8. Sequence diagram of the link between the target node and one anchor node.

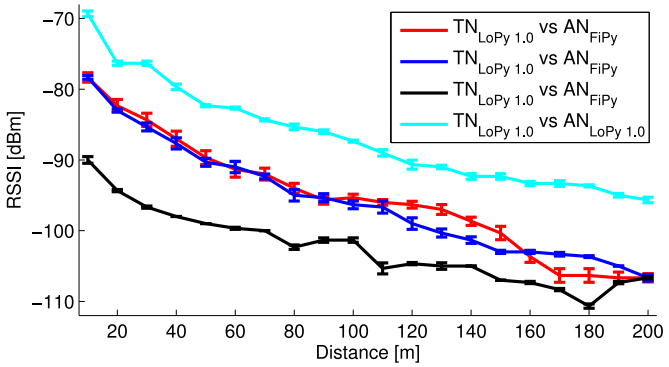

Fig. 9. The characteristic curve of the return link for the 90 m × 90 m scenario with $BW = 500$ kHz, $SF = 12$ y $P_{TX} = 5$ dBm.

node at a time, following a round-robin type procedure (Fig. 7). The aim of each link is to measure and store the value of the RSSI variable resulting of the communication between the target node and the respective anchor node. After that, using the RSSI-based positioning and the trilateration localization algorithm, we estimate the location of the target node.

There are three main components in the positioning system (see Fig. 7): the target node, the anchor nodes, and the main processor. We also identify two communication links: (1) The link between the target node and each of the anchor nodes using a LoRa interface to send request messages and to obtain relevant values such as RSSI and SNR. (2) The communication link between the target node and the processor through a WiFi interface. We use the FTP protocol to get the variable registers from the internal memory of the target node to the processor system.

The LoRa communication link between the target node and each anchor node follows the messages sequence shown in Fig. 8. The target node sends a request to one anchor node, identified with 1 byte of unique identity field included in the payload of the LoRa frame. Then, the anchor node with such identity sends a reply message. For the positioning system, the reply message corresponds to the return link and we also measure the RSSI value of this link.

6.2. Performance evaluation

The positioning system uses two relevant RSSI measurements on each link between the target node and the anchor nodes. Specifically, the RSSI value of the forward link measured by the anchor node, and the RSSI of the return link measured by the target node. In this way, we analyze the performance of the system under three different approaches. (1) The location of the target using only the RSSI of the forward link. (2) The location of the target using only the RSSI of the backward link. (3) The location of the target using the average RSSI value of the forward and return links.

The evaluation is based on field test measurements, carried out in the rural area of Pachamama in Cuenca-Ecuador ($2°49'58.72''S$; $78°55'43.75''O$). This is a flat land of around 500 × 500 m and all the communication links are with line of sight (LoS). Among others, we consider and report here the evaluation for two square area scenarios. One of 90 × 90 m, and the other of 150 × 150 m. In both cases we consider a symmetric distribution of four anchor nodes, one on each corner of the square.

Firstly, it is necessary to characterize each communication link between the target node and each of the anchor nodes. The aim is to obtain the path loss model of each link through a least squares adjustment of the RSSI values. For illustration purposes, Fig. 9 shows such resulting characterization for the return link of the 90 m × 90 m scenario. We follow a similar procedure for the forward link, the round trip link, and for the 150 × 150 m scenario.

6.2.1. Results analysis

One of the field measurement study was done in the 90 m × 90 m previously described scenario. We use four anchor nodes with identifiers *A, B, C* y *D* and fixed positions at the corners (0,0), (0,90), (90,90), (90,0) respectively. Table 4 summarizes the real position of the target node for five different test points. As previously said, we evaluate the performance of the positioning system for three different approaches: using only the RSSI value of the forward link, denoted by (e_1), the RSSI of the return link (e_2), and the average RSSI of the forward and return links (e_3). Since we use four anchor nodes, therefore, there are one useful estimation through the trilateration localization algorithm. On the other hand, it is important to note that if we use the RSSI information of just three of the anchor nodes for the trilateration algorithm, by combinatorics, there are $C_4^3 = 4$ possible useful position estimations. Then, we have a total of five valid possible position estimation for this reported test. We compute and select the centroid point of the whole set of estimations as the better approximation of the target position. As an illustration, Fig. 10 shows the whole set of five resulting estimations which are reported by our positioning system for one of the test points. Each of these are used to compute the centroid point as the better location approximation.

Table 4
Real position of the test points (x, y).

Scenario	P_1	P_2	P_3	P_4	P_5
90 m × 90 m	(35.35, 35.35)	(56.56,56.56)	(54.64,35.35)	(45,45)	(33.43,56.56)
150 m × 150 m	(63.63,63.63)	(84.85,84.85)	(86.36,63.63)	(75,75)	(65.14,84.85)

Table 5
Position estimation error.

Scenario	e_{link}	P_1	P_2	P_3	P_4	P_5	$\bar{e}$ (m)	(%)
90 m × 90 m	e_1 **(m)**	7.44	11.05	22.30	26.07	23.22	18.01	14.15
	$\boldsymbol{e_2}$ **(m)**	8.19	8.54	12.60	1.36	12.06	8.55	6.72
	$\boldsymbol{e_3}$ **(m)**	7.49	10.84	21.61	18.27	19.89	15.62	12.27
150 m × 150 m	e_1 **(m)**	9.57	10.74	10.96	13.59	15.66	12.11	5.70
	$\boldsymbol{e_2}$ **(m)**	19.03	18.04	12.96	22.91	29.85	20.56	9.69
	$\boldsymbol{e_3}$ **(m)**	12.69	14.18	11.73	22.91	22.19	16.74	7.89

In this context, we evaluate the accuracy of the system by means of the position estimation error, which in turn, is the distance between the real position and the estimated position of the target.

Table 5 summarizes the position estimation error of the system for each of the above described approaches. From these results, we can conclude that the use of the RSSI value of the return link presents a better approximation than the other two methods. In fact, the percentage of the average estimation error of this method is around the half of the error resulting with the other two methods.

Additionally, we evaluate the positioning system in a bigger area of 150 m × 150 m. We also use four anchor nodes located at the corners of this square area. Table 4 shows the real position of the target node for the five different test points. While Table 5 summarizes the position estimation error for this case. According to these results, and for this second scenario, we obtain a better accuracy using the RSSI information of the forward link. It is important to note that in no case the use of the average RSSI value of the forward and the return link present a better approximation. This is due to the great variability of each individual link and also of both links as a whole. It is also required to make a previous analysis of the behavior of the system for each operation scenario. This in order to define the more suitable approach which will result in the lesser localization error than the other approaches.

6.2.2. Simulation analysis

We complement the measurement-based evaluation of the system with a simulation-based analysis. The main objective is to predict the uncertainty resulting from the path loss model characterization of each link between the target and the anchor nodes, and the RSSI values of such links.

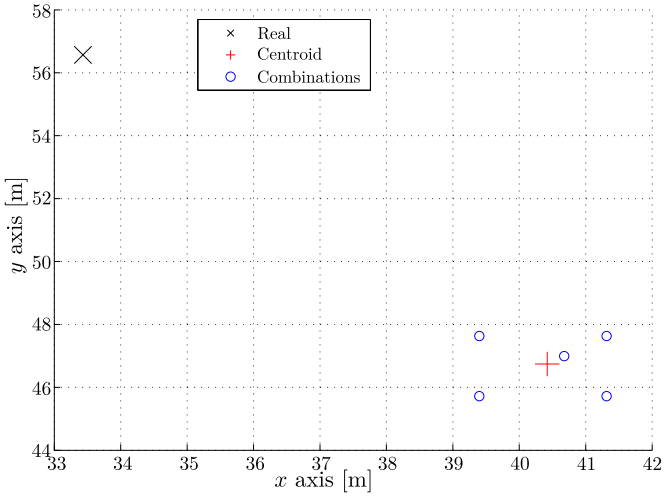

Fig. 10. Set of valid possible position estimations.

In order to be more reliable, we use the standard deviation of the RSSI variable obtained from the measurement-based characterization procedure (Fig. 9). We also utilize probabilistic distributions to establish a simulation set that allows to predict the behavior of the system for different locations of the target node.

Fig. 11 shows the resulting outputs of our system for ten different simulation tests. We evaluate one different location of the real points for each of the 60 × 60 m, 90 × 90 m, 150 × 150 m, and 200 × 200 m scenario.

Finally, for the 90 m × 90 m and 150 × 150 m scenarios, Fig. 12 shows the comparison of the position estimation error for the simulation results versus the evaluation based on real measurements. We observe an agreement between the simulation and the real measurements which validates our field test results.

We made additional field test evaluations including asymmetric scenarios and other rural zones around Cuenca city and the results are similar to the presented in this section.

6.2.3. Sources of uncertainty in positioning systems

Positioning system based on the RSSI variable has many sources of uncertainty that affect the measurements. This is mainly due to the influence of environmental factors, which cause radio frequency problems such: instability in the orientation of the antennas, transmission power variability, variability in RSSI sensitivity, among others. Some of the sources of uncertainty suffered in this work are:

- The measurements of the RSSI variable may vary by meteorological factors, that is, it could be different if the day is cloudy, sunny or rainy.
- Each antenna has its own radiation pattern that is not uniform. Therefore, a communication link between the anchor node and the target node can vary the RSSI measurement. It depends on the change in the orientation of the transmitter and receiver antennas.
- Based on the experimental evaluations carried out during this project, it can be affirmed that the FiPy and LoPy version 1.0 devices under the same LoRa configuration at the same P_{TX} have different behaviors in their real transmission powers. Therefore, RSSI measurements may be altered due to their internal manufacturing nature.
- Between the FiPy and LoPy devices there are different behaviors in their RSSI sensitivity. It happens under the same configuration parameters in LoRa modulation.
- If there are many transmitters operating at the same frequency in the measurement area. They can influence the measurements of the RSSI.

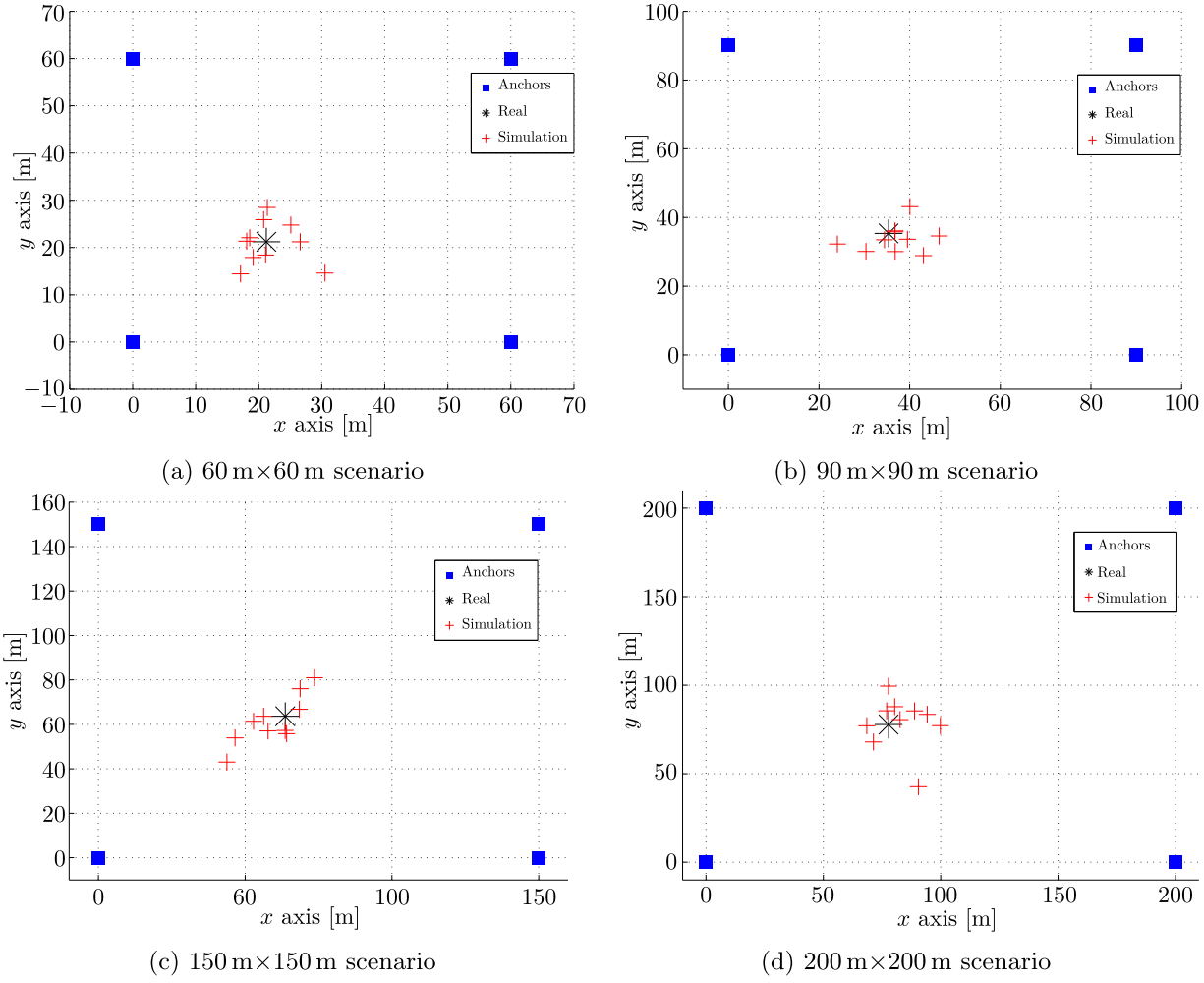

Fig. 11. Simulation results for different size scenarios.

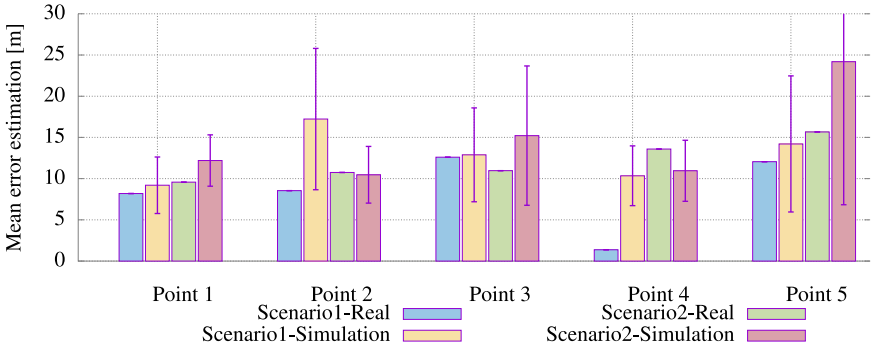

Fig. 12. Simulation errors versus real measurement errors.

- Current RSSI sensors have low resolution, that is, integer values in units of dBm, therefore they introduce quantization noise into the measurement.
- RSSI sensitivity is altered when the state of the power battery is discharged below a certain level.

7. Conclusions and future work

In this work, firstly, we have evaluated the Semtech LoRa devices regarding their time measurement capabilities, and the quality of their RF components. This evaluation focuses on the development of a low cost LoRa-based positioning system. Although with these devices we dispose of three options for the time measurement, the field test evaluation shows that no one of the RTT estimation methods are suitable for the development of a time-based positioning system such as ToA or TDoA. On the other hand, the evaluation of the quality of the RF components focuses on the RSSI sensitivity and dynamic range. We include the analysis of two versions of Semtech devices, i.e. LoPy 1.0 and FiPy. We observe that, although both kind of devices are based on the same SX1272 chip, they exhibit different RSSI behaviors. We also determine that the useful dynamic range for a RSSI-based positioning system is values of $RSSI > -110$ dBm. Since we are using a LPWAN technology, we really expect a wider dynamic range which would allow the positioning system to work in more extensive areas. Additionally, a deeper analysis of the real transmission power of the devices

shows that LoPy 1.0 power amplifier and accessories present better quality than the FiPy one.

On this basis, we develop a RSSI-based positioning system with the trilateration algorithm and we evaluate it by means of extensive field test on different rural scenarios and environment considerations. For this low cost system, we found on average a position estimation error of around 8.55 m corresponding to a error of 6.72% for the 90 m $\times$ 90 m square scenario. Meanwhile, for the 150 m $\times$ 150 m scenario the average error is around 12.11 m corresponding to a 5.70%.

Future research will include the evaluation and use of external RTC modules in order to be able to implement a time-based positioning system. We should also consider the use of different LoRa hardware implementations which present, at similar costs, better RSSI sensitivity and dynamic range. Temperature and humidity sensors should be included in the system, in order to determine the impact of the weather conditions over the RSSI values and its variability. Although our first objective is the evaluation of LoRa for outdoor positioning systems, we will include also the evaluation for indoor environments. Finally, we will evaluate alternative methods for solving the system of equations of the trilatearion algorithm such as minimum squares or Taylor series.

Declaration of Competing Interests

The authors declare that they have no known competing financial interests or personal relationships that could have appeared to influence the work reported in this paper.

Acknowledgments

This work was financed by the Research Department of the University of Cuenca (DIUC), Cuenca–Ecuador.

References

[1] R.U. Mondal, Radio frequency fingerprinting for outdoor user equipment localization, Jyväskylä Studies in Computing (271) (2017). https://jyx.jyu.fi/handle/123456789/56222.

[2] A. Savvides, C.-C. Han, M.B. Strivastava, Dynamic fine-grained localization in Ad-Hoc networks of sensors, in: Proceedings of the 7th Annual International Conference on Mobile Computing and Networking - MobiCom '01, ACM Press, Rome, Italy, 2001, pp. 166–179, doi:10.1145/381677.381693. http://portal.acm.org/citation.cfm?doid=381677.381693.

[3] S. Benaissa, D. Plets, E. Tanghe, J. Trogh, L. Martens, L. Vandaele, L. Verloock, F. Tuyttens, B. Sonck, W. Joseph, Internet of animals: characterisation of LoRa sub-GHz off-body wireless channel in dairy barns, Electronics Letters 53 (18) (2017) 1281–1283, doi:10.1049/el.2017.1344. http://digital-library.theiet.org/content/journals/10.1049/el.2017.1344.

[4] A.M. Baharudin, W. Yan, Long-range wireless sensor networks for geo-location tracking: Design and evaluation, in: 2016 International Electronics symposium (IES), IEEE, Denpasar, Indonesia, 2016, pp. 76–80, doi:10.1109/ELECSYM.2016.7860979. http://ieeexplore.ieee.org/document/7860979/.

[5] T. Sathyan, R. Shuttleworth, M. Hedley, K. Davids, Validity and reliability of a radio positioning system for tracking athletes in indoor and outdoor team sports, Behavior Research Methods 44 (4) (2012) 1108–1114, doi:10.3758/s13428-012-0192-2. http://www.springerlink.com/index/10.3758/s13428-012-0192-2.

[6] U. Raza, P. Kulkarni, M. Sooriyabandara, Low power wide area networks: an overview, IEEE Commun Surv Tut 19 (2) (2017) 855–873, doi:10.1109/COMST.2017.2652320.

[7] D. Patel, M. Won, Experimental study on low power wide area networks (LPWAN) for mobile internet of things, in: 2017 IEEE 85th Vehicular Technology Conference (VTC Spring), IEEE, Sydney, NSW, 2017, pp. 1–5, doi:10.1109/VTCSpring.2017.8108501. http://ieeexplore.ieee.org/document/8108501/.

[8] J.J. Kang, I. Khodasevych, S. Adibi, A disaster recovery system for location identification-based low power wide area networks (LPWAN), in: 2017 27th International Telecommunication Networks and Applications Conference (ITNAC), IEEE, Melbourne, VIC, 2017, pp. 1–6, doi:10.1109/ATNAC.2017.8215359. http://ieeexplore.ieee.org/document/8215359/.

[9] Sujuan Liu, Chuyu Xia, Zhenzhen Zhao, A low-power real-time air quality monitoring system using LPWAN based on LoRa, in: 2016 13th IEEE International Conference on Solid-State and Integrated Circuit Technology (ICSICT), IEEE, Hangzhou, China, 2016, pp. 379–381, doi:10.1109/ICSICT.2016.7998927. http://ieeexplore.ieee.org/document/7998927/.

[10] Sigfox, Sigfox, 2020. https://www.sigfox.com/.

[11] N.S. Knyazev, V.A. Chechetkin, D.A. Letavin, Comparative analysis of standards for low-power wide-area network, in: 2017 Systems of Signal Synchronization, Generating and Processing in Telecommunications (SINKHROINFO), IEEE, Kazan, Russia, 2017, pp. 1–4, doi:10.1109/SINKHROINFO.2017.7997528. http://ieeexplore.ieee.org/document/7997528/.

[12] O. Georgiou, U. Raza, Low Power Wide Area Network Analysis: Can LoRa Scale? IEEE Wireless Communications Letters 6 (2) (2017) 162–165, doi:10.1109/LWC.2016.2647247. http://ieeexplore.ieee.org/document/7803607/.

[13] B. Oniga, V. Dadarlat, E. De Poorter, A. Munteanu, Analysis, design and implementation of secure LoRaWAN sensor networks, in: 2017 13th IEEE International Conference on Intelligent Computer Communication and Processing (ICCP), IEEE, Cluj-Napoca, 2017, pp. 421–428, doi:10.1109/ICCP.2017.8117042. http://ieeexplore.ieee.org/document/8117042/.

[14] P. Neumann, J. Montavont, T. Noel, Indoor deployment of low-power wide area networks (LPWAN): A LoRaWAN case study, in: 2016 IEEE 12th International Conference on Wireless and Mobile Computing, Networking and Communications (WiMob), IEEE, New York, NY, 2016, pp. 1–8, doi:10.1109/WiMOB.2016.7763213. http://ieeexplore.ieee.org/document/7763213/.

[15] , Handbook of Position Location: Theory, Practice, and Advances, S.A.R. Zekavat, R.M. Buehrer (Eds.), John Wiley & Sons, Inc., Hoboken, NJ, USA, 2011, doi:10.1002/9781118104750.

[16] Iswandi, H.T. Nastiti, I.E. Praditya, I.W. Mustika, Evaluation of XBee-Pro transmission range for wireless sensor network's node under forested environments based on received signal strength indicator (RSSI), in: 2016 2nd International Conference on Science and Technology-Computer (ICST), IEEE, Yogyakarta, Indonesia, 2016, pp. 56–60, doi:10.1109/ICSTC.2016.7877347. http://ieeexplore.ieee.org/document/7877347/.

[17] T. Rama Rao, D. Balachander, A. Nanda Kiran, S. Oscar, RF propagation measurements in forest & plantation environments for wireless sensor networks, in: International Conference on Recent Trends in Information Technology, ICRTIT 2012, 2012, pp. 308–313, doi:10.1109/ICRTIT.2012.6206765.

[18] K. Mikhaylov, On the coverage of LPWANs: range evaluation and channel attenuation model for LoRa technology, in: ITS Telecommunications (ITST), 2015 14th International Conference on, 2016, pp. 55–59.

[19] A. Augustin, J. Yi, T. Clausen, W. Townsley, A Study of LoRa: ong Range & Low Power Networks for the Internet of Things, Sensors 16 (9) (2016) 1466, doi:10.3390/s16091466. http://www.mdpi.com/1424-8220/16/9/1466.

[20] Semtech, LoRa Modulation Basics, Technical Report, Semtech, 2015. http://www.semtech.com/images/datasheet/an1200.22.pdf.

[21] L. Vangelista, Frequency shift chirp modulation: the LoRa modulation, IEEE Signal Process Lett 24 (12) (2017) 1818–1821, doi:10.1109/LSP.2017.2762960.

[22] M. Bor, U. Roedig, LoRa Transmission Parameter Selection, in: Proceedings of the 13th IEEE International, 2017. http://www.research.lancs.ac.uk/portal/services/downloadRegister/164374357/lora_tps_r1342.pdf.

[23] M. Bor, J. Vidler, U. Roedig, Lora for the internet of things, in: Proceedings of the 2016 International Conference on Embedded Wireless Systems and Networks, 2016, pp. 361–366.

[24] P. Kulkarni, Q.O.A. Hakim, A. Lakas, Experimental evaluation of a campus-deployed IoT network using lora, IEEE Sens. J. 20 (5) (2020) 2803–2811, doi:10.1109/JSEN.2019.2953572.

[25] R. Fernandes, R. Oliveira, M. Luís, S. Sargento, On the real capacity of LoRa networks: the impact of non-destructive communications, IEEE Commun. Lett. 23 (12) (2019) 2437–2441, doi:10.1109/LCOMM.2019.2941476.

[26] J.M. Marais, R. Malekian, A.M. Abu-Mahfouz, Evaluating the LoRaWAN protocol using a permanent outdoor testbed, IEEE Sens. J. 19 (12) (2019) 4726–4733, doi:10.1109/JSEN.2019.2900735.

[27] G. Kazdaridis, S. Keranidis, P. Symeonidis, P. Tzimotoudis, I. Zographopoulos, P. Skrimponis, T. Korakis, Evaluation of LoRa performance in a City-wide testbed: experimentation insights and findings, in: Proceedings of the 13th International Workshop on Wireless Network Testbeds, Experimental Evaluation & Characterization, in: WiNTECH 19, Association for Computing Machinery, New York, NY, USA, 2019, pp. 29–36, doi:10.1145/3349623.3355474.

[28] W. Xu, J.Y. Kim, W. Huang, S.S. Kanhere, S.K. Jha, W. Hu, Measurement, characterization, and modeling of LoRa technology in multifloor buildings, IEEE Internet Things J. 7 (1) (2020) 298–310, doi:10.1109/JIOT.2019.2946900.

[29] D. Poluektov, M. Polovov, P. Kharin, M. Stusek, K. Zeman, P. Masek, I. Gudkova, J. Hosek, K. Samouylov, On the performance of LoRaWAN in smart city: end-device design and communication coverage, in: V.M. Vishnevskiy, K.E. Samouylov, D.V. Kozyrev (Eds.), Distributed Computer and Communication Networks, Springer International Publishing, Cham, 2019, pp. 15–29.

[30] T. Addabbo, A. Fort, M. Mugnaini, E. Panzardi, A. Pozzebon, V. Vignoli, A city-scale IoT architecture for monumental structures monitoring, Measurement 131 (2019) 349–357, doi:10.1016/j.measurement.2018.08.058. http://www.sciencedirect.com/science/article/pii/S0263224118307978.

[31] T. Hadwen, V. Smallbon, Q. Zhang, M. D'Souza, Energy efficient LoRa GPS tracker for dementia patients, in: 2017 39th Annual International Conference of the IEEE Engineering in Medicine and Biology Society (EMBC), IEEE, Seogwipo, 2017, pp. 771–774, doi:10.1109/EMBC.2017.8036938. https://ieeexplore.ieee.org/document/8036938/.

[32] B.C. Fargas, M.N. Petersen, GPS-free geolocation using LoRa in low-power WANs, in: 2017Global Internet of Things Summit (GIoTS), IEEE, Geneva, Switzerland, 2017, pp. 1–6, doi:10.1109/GIOTS.2017.8016251. http://ieeexplore.ieee.org/document/8016251/.

[33] Lora alliance, 2020. https://lora-alliance.org/.

[34] N. Podevijn, D. Plets, J. Trogh, L. Martens, P. Suanet, K. Hendrikse, W. Joseph, TDoA-Based Outdoor Positioning with Tracking Algorithm in a Public LoRa

Network, Wireless Communications and Mobile Computing 2018 (2018) 1–9, doi:10.1155/2018/1864209. https://www.hindawi.com/journals/wcmc/2018/1864209/.
[35] L. Sciullo, A. Trotta, M.D. Felice, Design and performance evaluation of a LoRa-based mobile emergency management system (LOCATE), Ad Hoc Networks 96 (2020) 101993, doi:10.1016/j.adhoc.2019.101993. http://www.sciencedirect.com/science/article/pii/S1570870518309004.
[36] R.S. Alonso, I. Sittón-Candanedo, Óscar García, J. Prieto, S. Rodríguez-González, An intelligent edge-IoT platform for monitoring livestock and crops in a dairy farming scenario, Ad Hoc Networks 98 (2020) 102047, doi:10.1016/j.adhoc.2019.102047. http://www.sciencedirect.com/science/article/pii/S1570870519306043.
[37] M.C. Vuran, A. Salam, R. Wong, S. Irmak, Internet of underground things in precision agriculture: Architecture and technology aspects, Ad Hoc Networks 81 (2018) 160–173, doi:10.1016/j.adhoc.2018.07.017. http://www.sciencedirect.com/science/article/pii/S1570870518305067.
[38] P. Avila-Campos, F. Astudillo-Salinas, A. Vazquez-Rodas, A. Araujo, Evaluation of LoRaWAN transmission range for wireless sensor networks in riparian forests, in: Proceedings of the 22nd International ACM Conference on Modeling, Analysis and Simulation of Wireless and Mobile Systems, in: MSWIM 19, Association for Computing Machinery, New York, NY, USA, 2019, pp. 199–206, doi:10.1145/3345768.3355934.
[39] M. Aref, A. Sikora, Free space range measurements with Semtech LoRa technology, in: Wireless Systems within the Conferences on Intelligent Data Acquisition and Advanced Computing Systems: Technology and Applications (IDAACS-SWS), 2014 2nd International Symposium on, 2014, pp. 19–23, doi:10.1109/IDAACS-SWS.2014.6954616.
[40] A.J. Wixted, P. Kinnaird, H. Larijani, A. Tait, A. Ahmadinia, N. Strachan, Evaluation of LoRa and LoRaWAN for wireless sensor networks, Proc IEEE Sens 0 (2017) 5–7, doi:10.1109/ICSENS.2016.7808712.
[41] L. Gregora, L. Vojtech, M. Neruda, Indoor signal propagation of LoRa technology, in: 2016 17th International Conference on Mechatronics - Mechatronika (ME), 2016, pp. 13–16.
[42] J. Petäjäjärvi, K. Mikhaylov, Evaluation of LoRa LPWAN technology for remote health and wellbeing monitoring, (ISMICT), 2016 10th..., 2016. http://ieeexplore.ieee.org/abstract/document/7498898/.
[43] W.C.Y. Lee, Estimate of local average power of a mobile radio signal, IEEE Trans. Veh. Technol. 34 (1) (1985) 22–27, doi:10.1109/T-VT.1985.24030.
[44] Pycom, Pycom. https://pycom.io/.
[45] Pycom, Datasheet FiPy, Datasheet, Pycom, 2018a. Versión 1.0. https://docs.pycom.io/.gitbook/assets/fipy-specsheet-1.pdf.
[46] Pycom, Datasheet LoPy versión 1.0, Datasheet, Pycom, 2018b. Versión 1.0. https://docs.pycom.io/.gitbook/assets/lopy-specsheet.pdf.
[47] Semtech, Semtech, 2020. https://www.semtech.com/.

Andres Vazquez-Rodas received the Electronics Engineering degree in 2004 from the Universidad Politécnica Salesiana Cuenca Ecuador, the Master degree in Telematics Engineering (Honors) from the Universidad de Cuenca Ecuador in 2010, and the Ph.D. from the Networking Department of the Universitat Politècnica de Catalunya BarcelonaTech (UPC), Spain in 2015. He was also an assistant professor at the Universidad Politécnica Salesiana until 2017. Since 2015 he is full time professor of the Universidad de Cuenca at the Electric, Electronic and Telecommunication Department (DEET) and the Engineering Faculty. His research interests include wireless mesh networks, wireless sensor networks, industrial networking and complex systems.

Darwin F. Astudillo-Salinas received the B.S.E (C.S) degree from Universidad de Cuenca, Cuenca, Ecuador, in 2007, and the M.S. and Ph.D. degrees from the Institut National Polytechnique de Toulouse, Toulouse, France, in 2009 and 2013, respectively. Since 2013, he has been a Full-Time Researcher with the Department of Electrical, Electronic, and Telecommunications Engineering, Universidad de Cuenca, Cuenca, Ecuador. His research interests include network coding, wireless sensor networks, vehicular networks, networked control systems, network simulation, network performance, cybersecurity and HPC.

Christian P. Sánchez Venenaula received his Electronics and Telecomunnication degree from the University of Cuenca, Cuenca Ecuador, in 2019. His research interests include wireless mesh networks, wireless sensor networks, network simulation, industrial networking, and cybersecurity.

Braulio Arpi received his Electronics and Telecomunnication degree from the University of Cuenca, Cuenca Ecuador, in 2019. His research interests include low power wide area networks, wireless sensor networks, network simulation, industrial networking, and cybersecurity.

Luis I. Minchala received the B.S.E.E. degree in electronics from the Salesian Polytechnic University, Cuenca, Ecuador, in 2006, and the M.S. and Ph.D. degrees in control engineering from Tecnológico de Monterrey, Monterrey, México, in 2011 and 2014, respectively. From summer 2012 to summer 2013, he was a Visiting Scholar at Concordia University, Montreal, QC, Canada. Between 2017–2018, he was a Postdoctoral Fellow at Tecnológico de Monterrey in the Climate Change Research Group. He is currently a full-time researcher with the Department of Electrical, Electronic and Telecommunications Engineering, Universidad de Cuenca, Ecuador. Dr. Minchala has authored and co-authored more than 40 indexed publications, including journal articles, conference proceedings, book chapters, and a book. His research interests are fault tolerant control applied to energy systems, automation and process control.